Journal of Solid Mechanics Vol. 11, No. 1 (2019) pp. 78-90
DOI: 10.22034/JSM.2019.664219

Smart Flat Membrane Sheet Vibration-Based Energy Harvesters

Y. Shahbazi *

Architecture and Urbanism Department, Tabriz Islamic Art University, Tabriz, Iran

Received 20 September 2018; accepted 13 December 2018

ABSTRACT

The dynamic responses of membrane are completely dependent on Pre-tensioned forces which are applied over a boundary of arbitrary curvilinear shape. In most practical cases, the dynamic responses of membrane structures are undesirable. Whilst they can be designed as vibration-based energy harvesters. In this paper a smart flat membrane sheet (SFMS) model for vibration-based energy harvester is proposed. The SFMS is made of an orthotropic polyvinylidene fluoride (PVDF) flat layer that has piezoelectricity effect. For this aim, polarization vector of PVDF layer is considered parallel to the applied electric field intensity vector. Electrodynamics governing equations of transverse motion of SFMS including active and modified pre-tensioned force are exploited. Transverse displacement component is expanded by the separable form corresponding to the axial and transverse and the linear ODE of motion based on generalized shape coefficients is obtained using Galerkin method. Finally, the explicit relation between forced vibration of SFMS and current and voltage harvesting are obtained. Numerical energy harvesting analyses were developed for an orthotropic rectangle SFMS and the voltage as function of the time is calculated based on different resistances. Parametric simulation shows a 1 m length and 0.5 width SFMS has ability to produce a peak to peak voltage about of 30 *mV*.

Keywords : Membrane; Smart structure; PVDF; Electrodynamics vibration, Energy harvesting.

1 INTRODUCTION

THE use of membranes and cables is increasing in aerospace, mechanic and civil engineering applications to achieve extremely large space structures such as antennas, telescopes, aircrafts, and solar concentrators. These structures are typically built with very light materials which are optimally used. The general form of the governing equations of the membrane theory of thin shells can also be found in [1]. A brief and useful historical review of theoretical and few experimental studies on membrane vibration have been published by [2]. In modern engineering a big effort is made to reduce the weight of structures. Reducing the weight bears advantages which lead to lower

*Corresponding author. Tel.: +98 41 35539207; Fax.: +98 41 35539200.
E-mail address: y.shahbazi@tabriziau.ac.ir (Y. Shahbazi).

manufacturing and operational costs and less required raw materials. However, light-weight structures tend to be more sensitive to static as well as dynamic instabilities. A solution to this problem without drastically changing the structural weight seems to be the implementation of smart materials to sense as well as to control the instabilities. An option which has been extensively investigated in recent years is the integration of piezoelectric patches or film in these mostly plate or shell-like structures. Piezoelectric materials belong to the so-called smart materials, or multi-functional materials, which have the ability to respond significantly to stimuli of different physical natures. If the coupling between the physical fields of different types has sufficient magnitude, the coupling can be used to build discrete or distributed transducers of various types, which can be used as sensors, actuators, or even integrated in structures with various degrees of tailoring and complexity (e.g. as fibers), to make them controllable or responsive to their environment (e.g. for shape morphing, precision shape control, damage detection, dynamic response. The direct piezoelectric effect consists in the ability of certain crystalline materials to generate an electrical charge in proportion to an externally applied force; the direct effect is used in force transducers. According to the inverse piezoelectric effect, an electric field parallel to the direction of polarization induces an expansion of the material [3]. In recent years, the development of energy harvesting from vibrating structures with piezoelectric sensors mounted on the surface has been a major focus of many research groups. Yipeng Wu et al. have presented the analytical expression of the harvested power based on a novel nonlinear energy extraction technique in which the harvested power is optimized whatever the connected load [4]. Furthermore, functionally graded piezoelectric materials with (FGPMs) are used as harvesting material. The properties of piezoelectric patches in FGPM layer change through the thickness direction. The theoretical and finite element investigations of FGPMs for shunted passive vibration damping of laminated composite beams have derived by M. Lezgy-Nazargah et al. [5]. They have determined optimal values of the electric components belonging to each shunt circuit. Several excellent review articles have been published the field of energy harvesting [6-10]. Other relevant studies include [11-15] have presented some special models of energy harvesters based on beam model. Most of previous studies have just considered a linear or nonlinear modelling of unimorph beams or plates. To the author's knowledge, the use of innovative linear and/or nonlinear structures other than unimorph beams or plates have not yet been considered satisfactorily. A dome-shaped model for piezoelectric micro machined ultrasonic transducer structure was proposed by Peng et al. [16]. Their results showed that a considerable improvement of electromechanical coupling performance was achieved with the dome-shaped model. Their research may be a motivation for new energy harvesting systems. Recently, Shahbazi et al. presented a new class of smart cylindrical membrane shell panel energy harvester for MEMS applications [17]. Despite comparison confirmed that their cylindrical membrane shell panel energy harvester could be a new perfect candidate for implementation in micro generators, the production of dome-shaped model in Micro and Nano scale will have difficulty.

Hence, in this paper, we try to present the electrodynamic governing equation and vibration amplitude to voltage harvesting relation of smart flat membrane sheet (SFMS) which can be used as a civil and architecture structure. For this aim, the Donnell's linear strain–displacement relationship and classical equilibrium equations of plane elasticity are used to obtain the system of coupled linear differential governing equation in terms of transverse displacement. The transverse function satisfying simply supported boundary conditions in the separable form corresponding to the axial and transverse are considered and the Galerkin method is applied to the governing electrodynamic equations which lead to a second-order ordinary linear differential equation. Finally, case studies are performed and the voltage generated with different resistance of SFMS energy harvester due to harmonic ambient vibration is simulated.

2 EQUATION OF MOTION OF SFMS FOR TRANSVERSE VIBRATIONS

2.1 Mathematical assumption

The SFMS is assumed to be stretched with sufficiently large stresses so that, if the subsequent transverse vibrational displacement is kept small, the stresses will remain essentially constant during vibration. In practice, this usually consists of stretching a membrane uniformly over a support frame. However, the tensile stress need not be uniform, and in reality it never is. Moreover, in-plane shear stresses, in addition to tensile stresses, may be applied at the membrane boundary. Such stresses are limited only by the requirement that at no point, and in no direction, within the membrane region will there be compressive stress. If a compressive stress component were to exist, the membrane would wrinkle because of its complete lack of bending stiffness.

In order to driving of governing electromechanical dynamics equations of motion, following assumptions are made:

- PVDF layer is considered orthotropic and are so arranged that at each point, its mutually orthogonal directions of elastic symmetry are coincided with *x*-*y* Cartesian coordinate.
- Transverse normal and shear strains, i.e. ε_z , ε_{xz} , and ε_{yz} are negligible.
- The applied electric field intensity is assumed to be distributed uniformly along the thickness direction.
- The polarization vector is assumed parallel to the applied electric field intensity vector both parallel to the thickness directions.
- The SFMS slopes at all points and in all directions are small during the vibratory motion.

The membrane strain components ε_{xx}^{z} , ε_{yy}^{z} , and γ_{xy}^{z} at an arbitrary point of the SFMS, at a distance *z* from middle surface, are related to the middle surface strains ε_{xx}^{0} , ε_{yy}^{0} , γ_{xy}^{0} and to changes in the curvature and torsion of middle surface χ_x , χ_y , and χ_{xy} by the following three relations:

$$\varepsilon_{xx}^{z} = \varepsilon_{x}^{0} + z\,\chi_x \qquad \varepsilon_{yy}^{z} = \varepsilon_{y}^{0} + z\,\chi_y \qquad \gamma_{xy}^{z} = \gamma_{xy}^{0} + z\,\chi_{xy} \tag{1}$$

The linear matrices of membrane strains associated with the displacement field of SFMS and the curvature changes are written as:

$$\begin{aligned} &\varepsilon_x^0 = \frac{\partial u}{\partial x} && \frac{\partial v}{\partial y} = \varepsilon_y^0 && \gamma_{xy}^0 = \frac{\partial u}{\partial y} + \frac{\partial v}{\partial x} \\ &\chi_x = -\frac{\partial^2 w}{\partial x^2} && \chi_y = -\frac{\partial^2 w}{\partial y^2} && \chi_{xy} = -2\frac{\partial^2 w}{\partial x\,\partial y} \end{aligned} \tag{2}$$

2.2 Piezoelectric constitutive equations

The constitutive equations for the Converse and Direct effects of SFMS can be written, as follows:

$$\begin{aligned} &\varepsilon_i = S_{ij}\sigma_j + d_{mi}E_m && \text{Converse Piezoelectric Effect} \\ &D_m = d_{mi}\sigma_i + \in_{mk}^{T} E_k && \text{Direct Piezoelectric Effect} \end{aligned} \tag{3}$$

In spite of mentioned assumptions i.e. ε_z , ε_{xz} , and ε_{yz} are negligible, so $[\varepsilon]_{3\times1}$, $[\sigma]_{3\times1}$, $[S]_{3\times3}$, $[d]_{3\times3}$, $[E]_{3\times1}$, $[D]_{3\times1}$, and $[\in]_{3\times3}$ are the membrane strain matrices, the membrane stress matrices, the compliance matrices, the piezoelectric strain constant matrices, the applied electric field vector, the electric displacement vector and the permittivity matrices, respectively. The electric field is applied only in *z*- direction here. Then, $E_x = E_\theta = 0$. It is worthwhile to notice that assuming the electric field as applied in *z*- direction, the strain will be generated in the *x* and *y* directions and $d_{33} = 0$. Since compliance $[S]$ of any material is the inverse of its stiffness $[Q]$, the converse effect Eq. (3) can be written as:

$$\begin{bmatrix} \sigma_x \\ \sigma_y \\ \tau_{xy} \end{bmatrix} = \begin{bmatrix} \sigma_{0x} \\ \sigma_{0y} \\ \tau_{0xy} \end{bmatrix} + [Q] \begin{bmatrix} \varepsilon_x^0 \\ \varepsilon_y^0 \\ \gamma_{xy}^0 \end{bmatrix} + z^i [Q] \begin{bmatrix} \chi_x \\ \chi_y \\ \chi_{xy} \end{bmatrix} - [Q] \begin{bmatrix} d_{31} \\ d_{32} \\ 0 \end{bmatrix} [E_z] \tag{4}$$

where, σ_{0x} , σ_{0y} , and τ_{0xy} are the initial normal and shear stress, respectively. These stress applied on a rectangle SFMS, as shown in Fig. 1, are related to initial force per unit length T_{0x} , T_{0y} , and T_{xy} as below:

$$\begin{bmatrix} T_{0x} \\ T_{0y} \\ T_{0xy} \end{bmatrix} = \int_{-\frac{h}{2}}^{\frac{h}{2}} \begin{bmatrix} \sigma_{0x} \\ \sigma_{0y} \\ \tau_{0xy} \end{bmatrix} dz = h \begin{bmatrix} \sigma_{0x} \\ \sigma_{0y} \\ \tau_{0xy} \end{bmatrix} \tag{5}$$

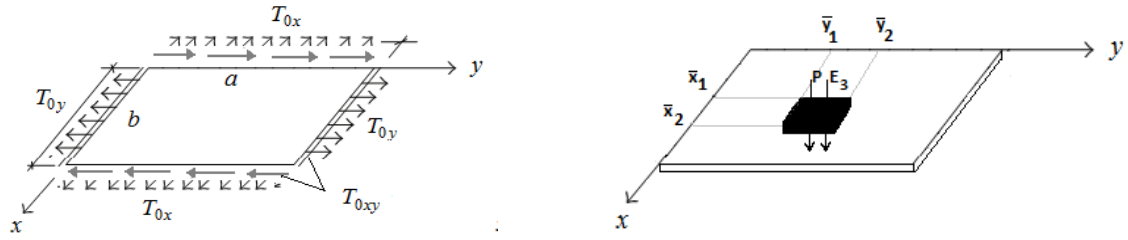

(a) (b)

Fig.1
Rectangular smart flat membrane sheet (SFMS). (a) Initial normal and shear stress for; (b) Polarization Direction and distribution of surface electrodes.

The SFMS is assumed orthotropic with following stiffness matrices $[Q]$:

$$[Q] = \begin{bmatrix} Q_{11} & Q_{12} & 0 \\ Q_{12} & Q_{22} & 0 \\ 0 & 0 & Q_{66} \end{bmatrix} \tag{6}$$

where, $Q_{11} = \dfrac{E_{xx}}{\left(1-\nu_{xy}^2\, E_{yy}/E_{xx}\right)}$, $Q_{12} = \dfrac{\nu_{xy} E_{yy}}{\left(1-\nu_{xy}^2\, E_{yy}/E_{xx}\right)}$, $Q_{22} = \dfrac{E_{yy}}{\left(1-\nu_{xy}^2\, E_{yy}/E_{xx}\right)}$, and $Q_{66} = G_{xy}$. In these expressions, E_{xx}, E_{yy}, ν_{xy}, and G_{xy} are the Young's modules, Poisson's ratio and Shear modules, respectively. It's worth mentioning that such stresses are limited only by the requirement that at no point, and in no direction, within the membrane region will there be compressive stress and the wrinkle will not occur.

The tension resultants of the membrane stresses $\bar{T}_x$, $\bar{T}_y$, and $\bar{T}_{xy}$ which are the total load acting per unit length of the middle surface of the SFMS can be calculated by the following integrations:

$$\begin{bmatrix} \bar{T}_x \\ \bar{T}_y \\ \bar{T}_{xy} \end{bmatrix} = \int_{-\frac{h}{2}}^{\frac{h}{2}} \begin{bmatrix} \sigma_x \\ \sigma_y \\ \tau_{xy} \end{bmatrix} dz = \int_{-\frac{h}{2}}^{\frac{h}{2}} \begin{bmatrix} \sigma_{0x} \\ \sigma_{0y} \\ \tau_{0xy} \end{bmatrix} dz + \int_{-\frac{h}{2}}^{\frac{h}{2}} \left([Q] \begin{bmatrix} \varepsilon_x^0 \\ \varepsilon_y^0 \\ \gamma_{xy}^0 \end{bmatrix} + z\,[Q] \begin{bmatrix} \chi_x \\ \chi_y \\ \chi_{xy} \end{bmatrix} \right) dz - \int_{-\frac{h}{2}}^{\frac{h}{2}} \left([Q] \begin{bmatrix} d_{31} \\ d_{32} \\ 0 \end{bmatrix} [E_z] \right) dz \tag{7}$$

By introducing the following matrices and vectors A_{rs}, B_{rs}, P_{r1}.

$$(A_{rs}, B_{rs}) = \int_{-\frac{h}{2}}^{\frac{h}{2}} [Q](1, z)\, dz \qquad r, s = x, y, z \tag{8}$$

$$P_{r1} = \int_{-\frac{h}{2}}^{\frac{h}{2}} \left([Q] \begin{bmatrix} d_{31} \\ d_{32} \\ 0 \end{bmatrix} [E_z] \right) dz \qquad r = x, y, z \tag{9}$$

Also, considering the $B = 0$ for single layer SMFS, The Eq. (7) will yield as:

$$\begin{bmatrix} \bar{T}_x \\ \bar{T}_y \\ \bar{T}_{xy} \end{bmatrix} = \begin{bmatrix} T_{0x} \\ T_{0y} \\ T_{0xy} \end{bmatrix} + \begin{bmatrix} A_{11} & A_{12} & 0 \\ A_{12} & A_{22} & 0 \\ 0 & 0 & A_{66} \end{bmatrix} \begin{bmatrix} \varepsilon_x^0 \\ \varepsilon_y^0 \\ \gamma_{xy}^0 \end{bmatrix} - \begin{bmatrix} P_x \\ P_y \\ 0 \end{bmatrix} \tag{10}$$

The Eq. (10) can be divided to initial, passive and active following stress resultant parts, namely:

$$\begin{bmatrix} \bar{T}_x \\ \bar{T}_y \\ \bar{T}_{xy} \end{bmatrix} = \begin{bmatrix} T_{0x} \\ T_{0y} \\ T_{0xy} \end{bmatrix} + \begin{bmatrix} T_x \\ T_y \\ T_{xy} \end{bmatrix} - \begin{bmatrix} P_x \\ P_y \\ 0 \end{bmatrix} \tag{11}$$

with the same calculation and based on mentioned assumptions, the direct piezoelectric effect can be written in its expanded form as:

$$D_z = d_{31}\sigma_x + d_{32}\sigma_y + \in_{zz} E_z \tag{12}$$

Substituting Eq. (5) in Eq. (12), the electrical displacement of SMFS can be written as function of stiffness components. Namely:

$$D_z = \begin{Bmatrix} d_{31}\sigma_{0x} + d_{32}\sigma_{0y} + \left(d_{31}Q_{11} + d_{32}Q_{12}\right)\varepsilon_x^0 + \left(d_{32}Q_{22} + d_{31}Q_{12}\right)\varepsilon_y^0 \\ +z\left(d_{31}Q_{11}\chi_x + d_{32}Q_{12}\right)\chi_x + z\left(d_{32}Q_{22}\chi_y + d_{31}Q_{12}\right)\chi_y \\ +\left(\in_{zz} - d_{31}{}^2Q_{11} - 2d_{31}d_{32}Q_{12} - d_{32}{}^2Q_{22}\right)E_z \end{Bmatrix} \tag{13}$$

The charge developed on the i^{th} electrode surface distributed between $\left[\bar{x}_1^i, \bar{x}_2^i\right]$ and $\left[\bar{y}_1^i, \bar{y}_2^i\right]$ can be expressed as the electrical displacement integral on the area of the surface. The charge expression in absence of inplane displacement components *u* and *v* can be written:

$$Q^i = \int_{\bar{x}_1^i}^{\bar{x}_2^i}\int_{\bar{y}_2^i}^{\bar{y}_2^i} D_z\,dxdy = \int_{\bar{x}_1^i}^{\bar{x}_2^i}\int_{\bar{y}_2^i}^{\bar{y}_2^i} \left\{ \begin{matrix} d_{31}\sigma_{0x} + d_{32}\sigma_{0y} + \left(d_{31}Q_{11} + d_{32}Q_{12}\right)\left(\dfrac{\partial u}{\partial x}\right) + \left(d_{31}Q_{12} + d_{32}Q_{22}\right)\left(\dfrac{\partial v}{\partial y}\right) \\ -z\left(d_{31}Q_{11} + d_{32}Q_{12}\right)\left(\dfrac{\partial^2 w}{\partial x^2}\right) - z\left(d_{31}Q_{12} + d_{32}Q_{22}\right)\left(\dfrac{\partial^2 w}{\partial y^2}\right) \\ +\left(\in_{zz} - d_{31}{}^2Q_{11} - 2d_{31}d_{32}Q_{12} - d_{32}{}^2Q_{22}\right)E_Z^i \end{matrix} \right\} dxdy \tag{14}$$

2.3 Electrodynamics equation of motion of SFMS

In this part, the electrodynamics equations of motion of SFMS are derived. For this aim, we have followed whatever have presented for a passive membrane structure [1].

Assume a SFMS which is stretched over boundary regions. The stress applied externally may vary along the boundary. A three-dimensional sketch of its middle surface in a typical displaced position with membrane stress resultants $\bar{T}_x$, $\bar{T}_y$, $\bar{T}_{xy}$ and their variations acting on each side of the element is shown in Fig. 2.

Assuming that the SFMS slopes at all points and in all directions are small during the vibratory motion. Summing forces in the transverse (*z*) direction leads to:

$$-\bar{T}_x \frac{\partial w}{\partial x}dy + \left(\bar{T}_x + \frac{\partial \bar{T}_x}{\partial x}dx\right)\left(\frac{\partial w}{\partial x} + \frac{\partial}{\partial x}\frac{\partial w}{\partial x}dx\right)dy - \bar{T}_y \frac{\partial w}{\partial y}dx + \left(\bar{T}_y + \frac{\partial \bar{T}_y}{\partial y}dy\right)\left(\frac{\partial w}{\partial y} + \frac{\partial}{\partial y}\frac{\partial w}{\partial y}dy\right)dx$$
$$-\bar{T}_{xy} \frac{\partial w}{\partial y}dy + \left(\bar{T}_{xy} + \frac{\partial \bar{T}_{xy}}{\partial x}dx\right)\left(\frac{\partial w}{\partial y} + \frac{\partial}{\partial x}\frac{\partial w}{\partial y}dx\right)dy - \bar{T}_{yx} \frac{\partial w}{\partial x}dx + \left(\bar{T}_{yx} + \frac{\partial \bar{T}_{yx}}{\partial y}dy\right)\left(\frac{\partial w}{\partial x} + \frac{\partial}{\partial y}\frac{\partial w}{\partial x}dy\right)dx \quad (15)$$
$$+q(x,y,t) = (\rho h dx dy)\frac{\partial^2 w}{\partial t^2}$$

where, ρ is mass density per unit volume of the material, and h is the membrane thickness. The harmonic pressure $q(x,y,t) = \bar{p}[H(x-x_1) - H(x-x_2)][H(y-y_1) - H(y-y_2)]\sin(\bar{\omega}t)$, having units of force/area, distributed over the surface of the membrane in domain $x_1 - x_2$ and $y_1 - y_2$. It's worth mentioning that such stresses may be applied on a specific surface of membrane in which the distribution should be presented using Heaviside function. By replacing $\bar{T}_x$ with its average value $\left\{\bar{T}_x + \left[\bar{T}_x + \left(\partial \bar{T}_x / \partial y\right)dy\right]\right\}/2$, and $\frac{\partial w}{\partial x}$ with its average value $\left\{\frac{\partial w}{\partial x} + \left[\frac{\partial w}{\partial x} + \frac{\partial(\partial w / \partial x)}{\partial y}dy\right]\right\}/2$, doing the same for $\bar{T}_y$, $\bar{T}_{xy}$, $\bar{T}_{yx}$, and $\frac{\partial w}{\partial y}$, and finally remaining just one and second order differential terms one obtains:

$$\frac{\partial}{\partial x}\left(\bar{T}_x \frac{\partial w}{\partial x}\right) + \frac{\partial}{\partial y}\left(\bar{T}_y \frac{\partial w}{\partial y}\right) + \frac{\partial}{\partial x}\left(\bar{T}_{xy} \frac{\partial w}{\partial y}\right) + \frac{\partial}{\partial y}\left(\bar{T}_{yx} \frac{\partial w}{\partial x}\right) + q(x,y,t) = \rho h \frac{\partial^2 w}{\partial t^2} \quad (16)$$

Summing moments about an axis parallel to *z*, and through the center of mass of the element shows that $\bar{T}_{xy} = \bar{T}_{yx}$. Also, summing forces in the *x* and *y* directions, and assuming that there are no significant accelerations or body forces (e.g., gravity, centrifugal) in the *x* and *y* directions, one obtains the following classical equilibrium equations of plane elasticity.

$$\frac{\partial\left(\bar{T}_x\right)}{\partial x} + \frac{\partial\left(\bar{T}_{xy}\right)}{\partial y} = 0 \quad (17)$$

$$\frac{\partial\left(\bar{T}_y\right)}{\partial y} + \frac{\partial\left(\bar{T}_{xy}\right)}{\partial x} = 0 \quad (18)$$

Multiplying Eq. (17) by $\frac{\partial w}{\partial x}$, and Eq. (18) by $\frac{\partial w}{\partial y}$, and then subtracting both from (16), the transversely electrodynamics equation of motion of SFMS becomes:

$$\bar{T}_x \frac{\partial^2 w}{\partial x^2} + 2\bar{T}_{xy} \frac{\partial^2 w}{\partial x \partial y} + \bar{T}_y \frac{\partial^2 w}{\partial y^2} + q(x,y,t) = \rho h \frac{\partial^2 w}{\partial t^2} \quad (19)$$

It is worth to mentioning that $\bar{T}_x$, $\bar{T}_y$, and $\bar{T}_{xy}$ are functions of *x*, *y*, and *t*. In following, we assumed that the initial stress resultants are sufficiently large that remain essentially unchanged due to the vibratory displacement. Also, the initial shear stress T_{0xy}, and active loads P_x, P_y are neglected. In spite of mentioned assumption, it can be written that $\left[\bar{T}_x \quad \bar{T}_y \quad \bar{T}_{xy}\right] = \left[T_{0x} \quad T_{0y} \quad 0\right]$.

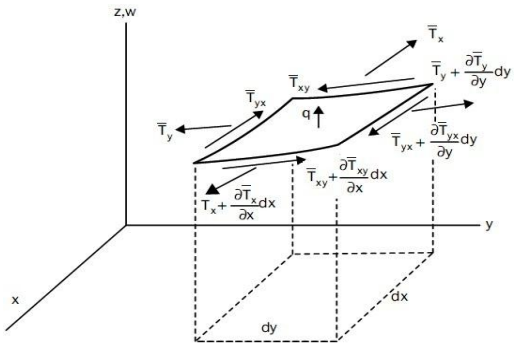

Fig.2
Stress resultants on infinitesimal SFMS element.

3 FORCED VIBRATION AND ENERGY HARVESTING ANALYSES

3.1 Mathematical formulation

In calculating of forced vibration response of the SFMS, deflection function $w\left(x,y,t\right)$ satisfying the boundary condition, Eq. (20), in the separable form corresponding to the axial and transverse wave numbers *i, j* can be written as:

$$w\left(x,y,t\right)=\sum_{m=1}^{\infty}\sum_{n=1}^{\infty}Z_{mn}\left(t\right)\sin\left(\alpha_m x\right)\sin\left(\beta_n y\right) \tag{20}$$

Here, $\alpha_m=\frac{m\pi}{a}$, $\beta_n=\frac{n\pi}{b}$, and $Z_{mn}\left(t\right)$ is the generalized coordinate that is unknown function of *t*. Form the orthogonality of the trigonometric function, it can be concluded that:

$$Z_{mn}\left(x,y,0\right)=\int_0^a\int_0^b w\left(x,y,0\right)\sin\left(\alpha_m x\right)\sin\left(\beta_n y\right)dxdy \tag{21}$$

$$\dot{Z}_{mn}\left(x,y,0\right)=\int_0^a\int_0^b \dot{w}\left(x,y,0\right)\sin\left(\alpha_m x\right)\sin\left(\beta_n y\right)dxdy \tag{22}$$

where $w\left(x,y,0\right)$ and $\dot{w}\left(x,y,0\right)$ are initial deflection and velocity of SMFS, respectively. Substituting the displacement function Eq. (20) into Eq. (19), we apply the Galerkin method; that is, each phrase of Eq. (19) multiplied by the corresponding special parts of the displacements in Eq. (20) and the result is integrated over the domain of the SFMS. Hence, the Eq. (19) will be changed to system of linear second-order ODEs in terms of the unknown time function $Z_{mn}\left(t\right)$, as below:

$$k_1\frac{\partial^2 Z_{mn}\left(t\right)}{\partial t^2}+k_2 Z_{mn}\left(t\right)=q_{mn}\sin(\bar{\omega}t) \tag{23}$$

where,

$$\begin{aligned} &k_1=\rho h \qquad k_2=\left(T_{0x}\alpha_m{}^2+T_{0y}\beta_n{}^2\right)\\ &q_{mn}=\frac{4\bar{p}}{ab\alpha_m\beta_n}\left[\cos\left(\alpha_m x_2\right)-\cos\left(\alpha_m x_1\right)\right]\left[\cos\left(\beta_n y_2\right)-\cos\left(\beta_n y_1\right)\right] \end{aligned} \tag{24}$$

The linear second-order differential Eq. (23) has following response:

$$Z_{mn}(t)=Z_{mn}(x,y,0)\sin\left(\sqrt{\frac{k_2}{k_1}}t\right)+\dot{Z}_{mn}(x,y,0)\left(\sqrt{\frac{k_2}{k_1}}t\right)-\frac{q_{mn}}{k_2-k_1\bar{\omega}^2}\sin(\bar{\omega}t) \tag{25}$$

Recalling Eq. (20), the deflection function $w(x,y,t)$ of SFMS can be written as:

$$w(x,y,t)=\sum_{i=1}^{\infty}\sum_{j=1}^{\infty}\left\{Z_{mn}(x,y,0)\sin\left(\sqrt{\frac{k_2}{k_1}}t\right)+\dot{Z}_{mn}(x,y,0)\left(\sqrt{\frac{k_2}{k_1}}t\right)-\frac{q_{mn}}{k_2-k_1\bar{\omega}^2}\sin(\bar{\omega}t)\right\}\sin(\alpha_m x)\sin(\beta_n y) \tag{26}$$

Assuming the uniform electric field E_Z^i can be expressed as $E_Z^i=-\frac{\partial V_i}{\partial z}=-\frac{V_i}{h_i}$, which the V_i is the potential difference between the upper and lower surface of the i^{th} distributed electrode. It is worthwhile to notice that the current, charge and voltage are all functions of the time. The frequency $\bar{\omega}$ of these periodic functions is dependent upon the external distributed load $q(x,y,t)$ applied to the SMFS. The amplitude of the current is that of the charge times the excitation frequency that is given as:

$$I(t)=\bar{\omega}Q(t) \tag{27}$$

The relation between voltage and current for an electrical circuit with pure resistance is expressed as:

$$I(t)=\frac{V(t)}{R} \tag{28}$$

Combining Eq. (13), (25), (26) and Eq. (27), the amplitude of the current for i^{th} distributed electrode can be determined as:

$$I^i(t)=\frac{\bar{\omega}\int_{\bar{x}_1^i}^{\bar{x}_2^i}\int_{\bar{y}_1^i}^{\bar{y}_2^i}\left\{-z\left(d_{31}Q_{11}+d_{32}Q_{12}\right)\left(\frac{\partial^2 w}{\partial x^2}\right)-z\left(d_{31}Q_{12}+d_{32}Q_{22}\right)\left(\frac{\partial^2 w}{\partial y^2}\right)\right\}dxdy}{1+\frac{\bar{\omega}R}{h}\int_{\bar{x}_1^i}^{\bar{x}_2^i}\int_{\bar{y}_1^i}^{\bar{y}_2^i}\left\{\left(\in_{zz}-d_{31}{}^2Q_{11}-2d_{31}d_{32}Q_{12}-d_{32}{}^2Q_{22}\right)\right\}dxdy} \tag{29}$$

Substituting $w(x,y,t)$ from Eq. (26) at rest condition in Eq. (29), integrating in domain $\left[\bar{x}_1^i,\bar{x}_2^i\right]$ and $\left[\bar{y}_1^i,\bar{y}_2^i\right]$, current for i^{th} distributed can be expressed as $I^i(t)=\frac{Num}{Den}$ in which:

$$\begin{aligned}Num&=\frac{z\,\bar{\omega}q_{mn}}{k_2-k_1\bar{\omega}^2}\left\{\begin{matrix}\frac{\alpha_m}{\beta_n}\left(d_{31}Q_{11}+d_{32}Q_{12}\right)\\+\frac{\beta_n}{\alpha_m}\left(d_{31}Q_{12}+d_{32}Q_{22}\right)\end{matrix}\right\}\left\{\left[\cos(\alpha_m\bar{x}_2^i)-\cos(\alpha_m\bar{x}_1^i)\right]\left[\cos(\beta_n\bar{y}_2^i)-\cos(\beta_n\bar{y}_1^i)\right]\right\}\sin(\bar{\omega}t)\\Den&=1+\frac{\bar{\omega}R}{h}\left(\in_{zz}-d_{31}{}^2Q_{11}-2d_{31}d_{32}Q_{12}-d_{32}{}^2Q_{22}\right).\left(\bar{x}_2^i-\bar{x}_1^i\right).\left(\bar{y}_2^i-\bar{y}_1^i\right)\end{aligned} \tag{30}$$

4 NUMERICAL ANALYSIS AND DISCUSSION

In following, the numerical energy harvesting analyses were developed for an orthotropic rectangle SFMS. The analyses have been performed with following dimensions and material properties: $a=1m$, $b=0.5m$, $h=2mm$, $\rho=1800\,kg/m^3$, $\sigma_y=5.2MPa$, $E_{xx}=2.7GPa$, $E_{yy}=2.5GPa$, $G_{xy}=0.53GPa$, $\nu_{xy}=0.326$, $d_{31}=23\times10^{-12}\,m/V$,

$d_{32}=2.3\times10^{-12}\ m/V$, and $\in_{33}=1.6\times10^{-8}\ F/m$. The SFMS is assumed has stretched with $0.6\sigma_y$. The simulation has done only for *m*=*n*=1. At first, the effect of the $\bar{\omega}$ on the maximum deflection is analyzed. The SFMS should be excited at fundamental natural frequency where it experiences the largest deflections and presents maximum energy harvesting. However, in order to have a behavior correctly described by a linear theory, the vibration amplitude of the SFMS must be of the order of 1/10 of the thickness, or smaller.

Hence, the SFMS is excited at the spectral frequencies including $\bar{\omega}=50,\ 100,\ 150,\ 288.6\ Hz$ and the maximum deflections in midpoint $x=\frac{a}{2},\ y=\frac{b}{2}$ of SFMS are calculated numerically using MATLAB software. The deflection function of midpoint in the considered spectral frequencies are shown in Fig. 3 to Fig. 6. In all simulation, the linear assumption is evaluated. Afterwards, the voltage as function of the time is calculated based on different resistances $0.1,\ 0.5,\ 1,\ 5\ k\Omega$. In this simulation, the electrodes distribution is assumed on the whole of SFMS layers, i.e. $\left[\bar{x}_1=0,\bar{x}_2=a\right]$ and $\left[\bar{y}_1=0,\bar{y}_2=b\right]$. To obtain the maximum voltage harvesting, the SFMS should be excited at the frequency which present maximum deflection i.e. fundamental natural frequency $\bar{\omega}=288.6\ Hz$.

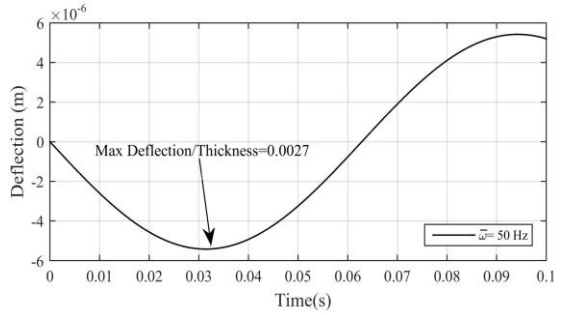

Fig.3
Forced vibration response of SFMS for $\bar{\omega}=50\ Hz$.

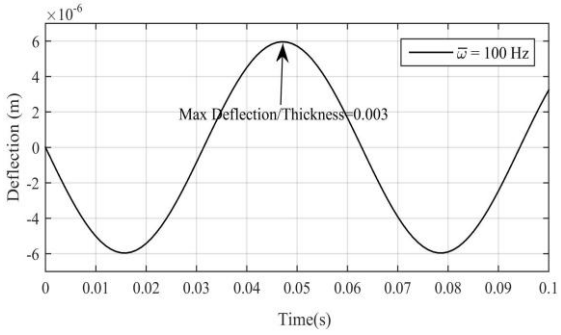

Fig.4
Forced vibration response of SFMS for $\bar{\omega}=100\ Hz$.

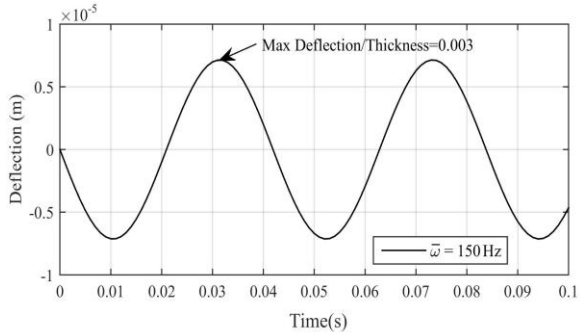

Fig.5
Forced vibration response of SFMS for $\bar{\omega}=150\ Hz$.

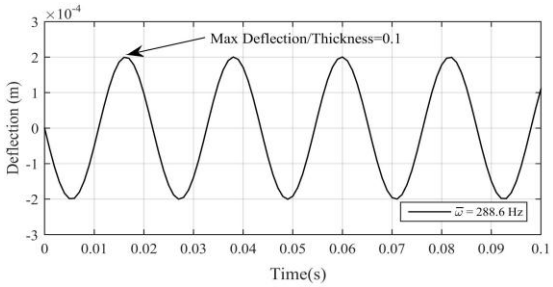

Fig.6
Forced vibration response of SFMS for $\bar{\omega} = 288.6\ Hz$.

The voltage harvesting for different resistances are illustrated in Fig. 7 to Fig. 10. It can be seen that a peak-to-peak voltage of 30 mV is produced.

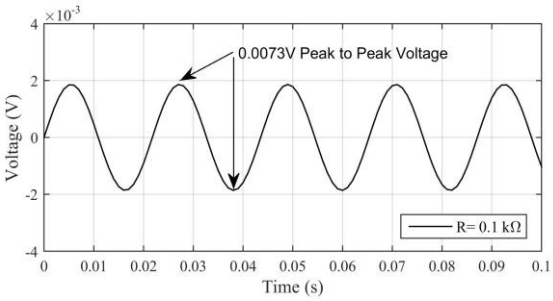

Fig.7
Amplitude of voltage harvesting as a function of the time for resistance $R = 0.1\ k\Omega$.

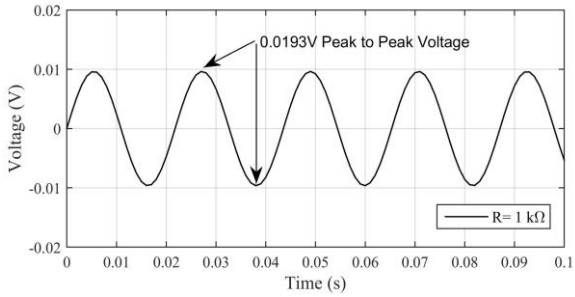

Fig.8
Amplitude of voltage harvesting as a function of the time for resistance $R = 0.5\ k\Omega$.

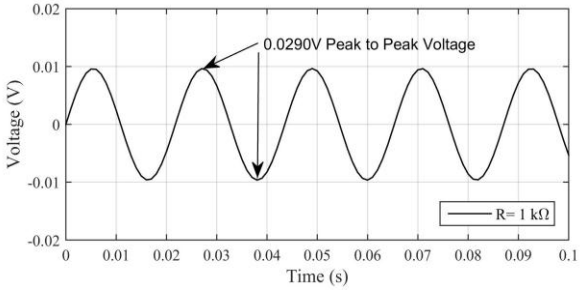

Fig.9
Amplitude of voltage harvesting as a function of the time for resistance $R = 1\ k\Omega$.

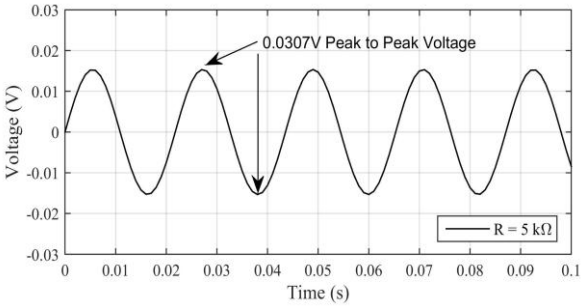

Fig.10
Amplitude of voltage harvesting as a function of the time for resistance $R = 5\ k\Omega$.

According to Eq. (26), Eq. (29) and Eq. (3), it may be concluded that the peak to peak voltage harvesting is depended on forced vibration frequency and vibration amplitude of SFMS. The control of forced vibration frequency is illogical while the vibration amplitude which itself is effected by the influence of pretension forces and linear displacement assumption may be increased. The more voltage harvesting may be obtained where the SFMS have low pretention forces or large nonlinear amplitude vibration occurred. For later state i.e. large nonlinear amplitude vibration, the nonlinear displacement assumption should be considered in formulation.

Finally, substituting Eq. (29) to Eq. (28), the voltage harvesting time domain function can be calculated as homographic functions or linear fractional transformations in general form $V(R)=\frac{a_1.R+b_1}{a_2.R+b_2}$. Where,

$$
\begin{aligned}
a_1 &= \bar{\omega}\int_{\bar{x}_1^i}^{\bar{x}_2^i}\int_{\bar{y}_1^i}^{\bar{y}_2^i}\left\{-z\left(d_{31}Q_{11}+d_{32}Q_{12}\right)\left(\frac{\partial^2 w}{\partial x^2}\right)-z\left(d_{31}Q_{12}+d_{32}Q_{22}\right)\left(\frac{\partial^2 w}{\partial y^2}\right)\right\}dxdy \\
b_1 &= 0 \\
a_2 &= \frac{\bar{\omega}}{h}\int_{\bar{x}_1^i}^{\bar{x}_2^i}\int_{\bar{y}_1^i}^{\bar{y}_2^i}\left\{\left(\in_{zz} -d_{31}{}^2Q_{11}-2d_{31}d_{32}Q_{12}-d_{32}{}^2Q_{22}\right)\right\}dxdy \\
b_2 &= 1
\end{aligned}
\tag{31}
$$

By introducing $\Delta=\begin{vmatrix}a_1 & b_1\\ a_2 & b_2\end{vmatrix}$ and considering above coefficients, it can be seen that $\Delta\langle 0$. For $\Delta\langle 0$ the values of the function are decreasing from ∞ to $\frac{a_1}{a_2}$. So, the minimum voltage harvesting based on different values of R is equal to $\frac{a_1}{a_2}$. While, the maximum voltage harvesting has no finite value.

Finally, the SFMS is compared with other recent energy harvester systems including beam, plate and membrane models. Shahbazi et al. have comprehensively discussed their smart cylindrical membrane shell panel harvester by nine recent studies of beam and plate models. They have also listed the target points geometrical design, frequency operation and output power or voltage of each work. The SFMS energy harvester is added to their table for a quantitative comparison of the SFMS's efficiency with previous projects. The comparison is presented in Table 1.

Table 1
Comparative performance of SFMS with of previous works reviewed by (Shahbazi et al. 2012).

Previous work	Design	Resonant frequency	Output power or voltage Fabrication
Work 1. MEMS based piezoelectric power generator array for vibration energy harvesting (Liu et al. 2008)	Cantilever size: Length = 2,000– 3,500 μm Width =750–1000 μm	226–234 *Hz d*31 mode	Output voltage of 3.93 *V DC*, Output power of 3.98 μW
Work 2. Energy Harvesting MEMS device based on thin film piezoelectric cantilevers (Choi et al. 2006)	Cantilever size: Length = 170 μm Width = 260 μm	3 mode: 13.9, 21.9 48.5 *kHz*	Output voltage of 2.4 *V* at 5.2 *MΩ* load Output power of 1.01 μW
Work 3. A free standing thick film piezoelectric energy harvester (Kok et al. 2008)	Cantilever size: Length = 13.5 *mm* Width = 9*mm* Thickness = 192 μm	229 *Hz d*31 mode	Output voltage of 130 *mV* Output Power of 270 *nW* at 9.81 m/s^2
Work 4. Two layered piezoelectric bender devices for micro power generator (Jeong et al. 2008)	Cantilever size: Length = 10 *mm* Width = 10 *mm*	120 *Hz*	Peak-to-peak voltage of 2.0 *V* and a power of 0.5 *mW* in resonance mode
Work 5. Piezoelectric scavengers in MEMS technology: fabrication and simulation (Schmitz et al. 2005)	The piezoelectric generator is located on top of the beam and consists piezoelectric layer sandwiched between top and bottom electrode	300–1000 *Hz* Variation of resonance frequencies: 300, 700, 1000 *Hz*	1–100 μW
Work 6. Piezoelectric harvesters and MEMS technology (Renaud et al. 2007)	The device is packages using two wafers	1.8 *kHz*	40 μW

Work 7. Laser machined piezoelectric cantilevers for mechanical energy harvesting (Hyunuk et al. 2008)	10 cantilevers on both side of the bridge, 5 of them are placed with tip mass alternately. Width = 4*mm* Length = 5.75 *mm*	870 *Hz*	Output power of 1.13 μW Power density of 301.3 $\mu W/cm^3$
Work 8. Power Harvesting Using Piezoelectric MEMS Generator with Interdigital Electrodes (Lee et al. 2007)	Cantilever size: Length = 3,000 μm Width = 1,500 μm Thickness = 22 μm	570–575 *Hz*	Output voltage of 1.127*VP-P*, Output power of 0.123 μW
Work 9. Power Harvesting Using Piezoelectric MEMS Generator with Interdigital Electrodes (Lee et al. 2007)	2 PVDF layers on both side of Epoxy core Length = 5000 μm Circumferential width= 0.001 *rad* Thickness of Epoxy layer= 100 μm Thickness of each PVDF layer=10 μm	471.79 *Hz*	Output voltage of 0.3204 *VP-P*, Output power of 0.467 μW
Work 10. Power Harvesting Using smart cylindrical membrane shell panel (Shahbazi et al. 2012)	2 PVDF layers on both side of Epoxy core Length = 5000 μm width= 0.001 *rad* Thickness of Epoxy= 100 μm Thickness of PVDF =10 μm	471.79 *Hz*	Output voltage of 0.3204 *VP-P*, Output power of 0.467 μW
proposed energy harvester: SFMS	$a = 1m$, $b = 0.5m$, $h = 2mm$	288.6 *Hz*	Output voltage of 0.0307 *VP-P*

5 CONCLUSIONS

In this study, electromechanical equations of motion and vibration to voltage harvesting relation of smart flat membrane sheet (SFMS) energy harvester are presented. The SFMS is PVDF laminate with piezoelectricity effect. The sensing and actuation mechanism are applied in piezoelectricity relations of SFMS. For this aim, polarization vector is parallel to the applied electric field intensity vector both parallel to the transverse directions. By assuming a series form function for displacement and inserting in equations without presence of external load and applying Galerkin method, the linear ordinary differential equation (ODE) of motion based on generalized shape coefficients is obtained. Finally, the explicit relation between vibration amplitude and voltage are calculated. Parametric simulation shows that a 1 *m* length and 0.5 width SFMS has ability to produce a peak to peak voltage about of $30mV$. The proposed harvester model efficiency is compared to with other recent energy harvester systems including beam, plate and cylindrical membrane models. The SFMS model, while easy to implement, has an acceptable efficiency.

ACKNOWLEDGEMENTS

This paper is a part of research study has been done in architecture and urbanism department of Tabriz Islamic Art University. The author would like to thank the Tabriz Islamic Art University for its financial support.

REFERENCES

[1] Leissa Arthur W., Qatu Mohamad S., 2011, *Vibration of Continuous Systems*, McGraw-Hill Education.
[2] Jenkins Christopher H.M., Korde Umesh A., 2006, Membrane vibration experiments: An historical review and recent results, *Journal of Sound and Vibration* **295**: 602-613.
[3] Preumont A., 2006, *Mechatronics Dynamics of Electromechanical and Piezoelectric Systems Materials*, Springer, Printed in the Netherlands.
[4] Yipeng W., Badel A., Formosa F., Liu W., Agbossou A. E., 2012, Piezoelectric vibration energy harvesting by optimized synchronous electric charge extraction, *Journal of Intelligent Material Systems* **24**(12): 1445-1458.
[5] Lezgy-Nazargah M., Divandar S.M., Vidal P., Polit O., 2017, Assessment of FGPM shunt damping for vibration reduction of laminated composite beams, *Journal of Sound and Vibration* **389**: 101-118.
[6] Priya S., 2007, Advances in energy harvesting using low profile piezoelectric transducers, *Journal of Electroceramics* **19**:165-182.

[7] Anton S.R., Sodano H.A., 2007, A review of power harvesting using piezoelectric materials (2003–2006), *Smart Materials and Structures* **16**: R1–R21.
[8] Beeby S.P., Tudor M.J., White N.M., 2006, Energy harvesting vibration sources for microsystems applications, *Measurement Science and Technology* **17**: R175–R195.
[9] Roundy S., Wright P.K., 2004, A piezoelectric vibration based generator for wireless electronics, *Smart Materials and Structures* **13**: 1131-1142.
[10] Sodano H., Inman D.J., Park G., 2004, A review of power harvesting from vibration using piezoelectric materials, *The Shock and Vibration Digest* **36**: 197-205.
[11] Erturk A., Inman D.J., 2008, Issues in mathematical modeling of piezoelectric energy harvesters, *Smart Materials and Structures* **17**(6): 065016.
[12] Erturk A., Inman D.J., 2009, An experimentally validated bimorph cantilever model for piezoelectric energy harvesting from base excitation, *Smart Materials and Structures* **18**(2): 025009.
[13] Priya S., Inman D.J., 2009, *Energy Harvesting Technologies*, Springer, New York.
[14] Goldschmidtboeing F., Woias P., 2008, Characterization of different beam shapes for piezoelectric energy harvesting, *Journal of Micromechanics and Microengineering* **18**: 104013.
[15] Guyomar D., Badel A., Lefeuvre E., Richard C., 2005, Toward energy harvesting using active materials and conversion improvement by nonlinear processing, *IEEE Transactions on Ultrasonics, Ferroelectrics and Frequency Control* **52**(4): 584-595.
[16] Peng J., Chao C., Tang H., 2010, Piezoelectric micromachined ultrasonic transducer based on dome-shaped piezoelectric single layer, *Microsystem Technologies* **16**: 1771-1775.
[17] Shahbazi Y., Chenaghlou M. R., Abedi K., Khosrowjerdi M. J., Preumont A., 2012, A new energy harvester using a cross-ply cylindrical membrane shell integrated with PVDF layers, *Microsystem Technologies* **18**: 1981-1989.